SCIENCE CHINA
Life Sciences

• RESEARCH PAPERS •

September 2011 Vol.54 No.9: 854–862
doi: 10.1007/s11427-011-4209-3

Global effect of an RNA polymerase β-subunit mutation on gene expression in the radiation-resistant bacterium *Deinococcus radiodurans*

HUA XiaoTing[1,2], WANG Hu[2], WANG Chao[2], TIAN Bing[2] & HUA YueJin[2*]

[1]*Department of Infectious Diseases, Sir Run Run Shaw Hospital, College of Medicine, Zhejiang University, Hangzhou 310016, China;*
[2]*Key Laboratory for Nuclear-Agricultural Sciences of the Chinese Ministry of Agriculture and Zhejiang Province, Institute of Nuclear-Agricultural Sciences, Zhejiang University, Hangzhou 310029, China*

Received March 15, 2011; accepted June 24, 2011; published online August 2, 2011

The β-subunit of RNA polymerase, which is involved in rifampin binding, is highly conserved among prokaryotes, and Rif^r mutants detected in many bacteria are the result of amino acid changes. Spontaneous rifampin resistance mutations resulting in amino acid replacement (L420R) and deletion (1258-66 9 bp deletion) have been previously isolated in the *rpoB* gene of *Deinococcus radiodurans*. In this study, a β-subunit mutation in *D. radiodurans* resulted in a unique effect on growth rate. We used DNA microarrays and biochemical assays to investigate how the Rif^r mutation in the β-subunit led to changes in growth rate via altered regulation of multiple genes. The expression of genes with predicted functions in metabolism, cellular processes and signaling, and information storage and processing were significantly altered in the 9 bp-deletion *rpoB* mutant. The consensus promoter sequence of up-regulated genes in the 9 bp-deletion *rpoB* mutant was identified as an AT-rich sequence. Greater levels of reactive oxygen species accumulated in the L420R and 9 bp-deletion *rpoB* mutants compared with wild type. These results provide insight into the molecular mechanism of how the β-subunit Rif^r mutation alters the regulation of multiple genes.

***rpoB*, rifampin, *Deinococcus*, transcriptome, microarray**

Citation: Hua X T, Wang H, Wang C, *et al*. Global effect of an RNA polymerase β-subunit mutation on gene expression in the radiation-resistant bacterium *Deinococcus radiodurans*. Sci China Life Sci, 2011, 54: 854–862, doi: 10.1007/s11427-011-4209-3

A genetic system for analyzing base substitutions has been developed in *D. radiodurans* and other bacteria, based on sequencing *rpoB* mutations that generate the rifampin-resistant (Rif^r) phenotype [1–3]. The β-subunit of RNA polymerase, which is involved in rifampin binding, is highly conserved among prokaryotes, and Rif^r mutants are the result of amino acid changes [1]. Analysis of the specificity of mutators and mutagens using the genetic system may lead to insight into the nature of mutagenesis and repair [2]. The system has been used to determine the mutation rates and mutation spectra of many mutators in *D. radiodurans*, such as *uvrD*, *mutS1*, *mutS2*, *mutS1 mutS2*, *mutL*, *zwf*, *zwf mutS1*, *recQ*, *uvrA1 uvrA2*, *uvrA1 uvrA2 uvsE*, *uvrA1*, *uvrA2*, *uvsE* and *recQ* [2,4–7].

There are fundamental connections between rifampin resistance, RNA polymerase structure and function and global gene expression. Rifampin can specifically block transcription initiation but not elongation [8]. Rif^r mutations in *Escherichia coli* can affect a wide variety of phenotypes, including altered growth properties and stimulated secondary metabolism [9]. Recently, a novel *rpoB* mutation in *Bacillus subtilis* showed a unique spectrum of effects on growth and various developmental events [10]. An *rpoB* mutation in *Streptomyces lividans* activated antibiotic pro-

*Corresponding author (email: yjhua@zju.edu.cn)

duction and reduced growth rate, and gene expression analysis demonstrated that the *rpoB* mutation elevated expression of pathway-specific regulatory genes independent of guanosine tetraphosphate (ppGpp) [11]. A spontaneous Rif^r mutation isolated from *Saccharopolyspora erythraea* stimulated bacterial secondary metabolism or caused slow-growth and was severely impaired in erythromycin production. DNA microarray analysis showed that this Rif^r mutation greatly changed the transcriptional profile of *S. erythraea* [12].

The RNA polymerase complex can contact every promoter in the genome, thus any change in critical portions of the enzyme can lead to global changes in gene transcription and hence in physiology and metabolism. Mutations within the Rif binding pocket of the β-subunit may alter the structure of RNA polymerase and hence its regulated interaction with specific promoters [13]. We have previously isolated Rif^r mutants from *D. radiodurans* [14]. In this study, the Rif^r mutants having a higher minimal inhibitory concentration (MIC) of rifampin resulted in slow growth. We used DNA microarrays to identify the individual promoter-RNA polymerase interactions that led to the change in growth rate in the *D. radiodurans* Rif^r mutant.

1 Materials and methods

1.1 Bacterial strains, media and antibiotics

All *D. radiodurans* cultures were grown at 30°C in TGY media (0.5% bacto tryptone, 0.1% glucose, 0.3% bacto yeast extract) with aeration or on TGY plates supplemented with 1.5% agar (Table 1). Rifampin was purchased from Xiamen Sanland Chemicals (Xiamen, China), and dissolved in dimethyl sulfoxide, which was purchased from Sigma (St. Louis, MO, USA).

1.2 Measurement of growth characteristics

1.2.1 Growth curves

Growth curves were determined in microtiter plates containing 200 μL of culture per well using a SpectraMax M5 Microplate Reader with SoftMax Pro Software (Molecular Devices) [15]. Overnight cultures were washed and diluted 100-fold in LB medium and pipetted (200 μL) into the wells of a microtiter plate. The optical density at 600 nm was measured every 5 min for 24 h. Before every measurement, the plate was shaken for a period of 30 s to ensure aerobic growth conditions. Each experiment was repeated three times.

1.2.2 Doubling-time measurement

Growth measurement was performed as described previously [16]. Briefly, 500 μL overnight culture of each strain was transferred to 50 mL of TGY. The culture was grown at 30°C with shaking at 250 r min^{-1}. The cultures were spread onto TGY agar plates after 2 h (t_1) and 4 h (t_2). The plates were incubated at 30°C for 3 d, and the number of Colony Forming Units (CFU) was determined. The doubling time (g) was calculated from $g=\ln 2/[(\log_{10}N_2-\log_{10}N_1)2.303/\Delta t]$, where N_1 is CFU mL^{-1} at t_1 and N_2 is CFU mL^{-1} at t_2.

1.2.3 Measure the diameter of D. radiodurans clones

Cells were harvested in early stationary phase and washed twice with and resuspended in the phosphate buffer (PB; 20 mmol L^{-1}, pH 7.4). After dilution with PB, the cells were plated on TGY plates and incubated at 30°C for 5 d. The diameters of the clones were measured daily.

1.3 RNA isolation, probe preparation, microarray hybridization and data analysis

Total RNA was extracted from 50 mL of *D. radiodurans* cultures using TRIZOL Reagent (Invitrogen, Carlsbad, CA, USA) following liquid nitrogen grinding. Each RNA sample was treated with 10 units of RNase free DNase I (Promega, Mannheim, Germany) and purified using phenol-chloroform extraction. RNA quality and quantity were evaluated by 1.0% formaldehyde denaturing agarose gel electrophoresis and by absorbance readings at 260 and 280 nm using a NanoDrop ND-1000 Spectrophotometer (NanoDrop, Wilmington, DE, USA).

Microarray preparation and hybridization were performed as published [17]. Briefly, 3156 pairs of 70-mer gene specific oligonucleotide probes were designed by Oligoarray software [18] and synthesized by Invitrogen (Shanghai, China). Each probe was printed twice on each array. Because of high variability in microarray hybridization, two replicated samples were prepared, and the RNA from each sample was hybridized with dye-swap. Thus, eight data points were available for each experiment.

GenePix pro 5.1 was used to quantify the hybridization signals. Normalization and statistical analyses were carried out in the R computing environment using the linear models for microarray data package (Limma) [19]. Prior to channel normalization, microarray outputs were filtered to remove spots of poor signal quality by excluding those data points with a mean intensity less than two standard deviations above background in both channels. Within Limma, global LOWESS normalization was carried out for each microarray [20], and the within-array correlation method was used to average the replicate spots [21]. In this study, we compared wild type with an *rpoB* mutant (1258-66 9 bp-deletion). Two independent cell cultures were prepared and used as biological replicas. The microarray data have been deposited in the Gene Expression Omnibus Database under accession No. GSE18661.

1.4 Real-time quantitative PCR

Twelve genes were chosen for real-time quantitative PCR. Among them, DR0089, a gene whose expression is unaffected by H_2O_2 and ionizing radiation, was regarded as a normalization factor. In short, first-strand cDNA synthesis was carried out in 20 μL of reaction mixture, containing 1 μg of each DNase I treated and purified total RNA sample, combined with 3 μg of random hexamers. The real-time PCR amplification used the BioEasy SYBR Green I Real Time PCR kit (BioFlux, Hangzhou, China) following the manufacturer's instructions. All assays were performed using Stratagene Mx3005P (Stratagene, Cedar Creek, TX, USA).

1.5 Motif analysis

The promoter sequences of repressed or induced genes were analyzed using the program MEME [22], with search parameters set to look for enriched motifs of 6–50 nucleotides in length, assuming sites were present once per sequence or not at all. E-box motifs identified by MEME were analyzed by the program WebLogo [23] to generate sequence logos.

1.6 Measurement of intracellular reactive oxygen species (ROS) levels

Luminol-enhanced chemiluminescence assays were used to measure intracellular ROS levels. Cells were harvested in the early stationary phase and washed twice with and re-suspended in phosphate-buffered saline (PBS). The luminol assay was performed by incubating cells in 1 mg mL^{-1} luminol in PBS and measuring luminescence using a Berthold Sirius luminometer [24]. Wild type and two *rpoB* mutants were independently measured three times.

2 Results

2.1 Mutants grew more slowly than the wild type

Growth curves were used to investigate the fitness of mutant strains. Mutant strains grew more slowly than the wild type in liquid and solid cultures (Figure 1A and B). Doubling-time of strains indicated the fitness of mutant strains; the fitness of R21 was approximately 0.73, and that of R20 was approximately 0.43 (Figure 1C).

2.2 The 9 bp-deletion *rpoB* mutant showed many basal gene expression changes compared with wild type

We determined the global gene expression patterns in two *D. radiodurans* strains using oligonucleotide microarrays. Gene expression changes in the 9 bp-deletion *rpoB* mutant were given as signal log ratios (mutant/wild type, log base 2), and ANOVA was used to compare gene expression lev-

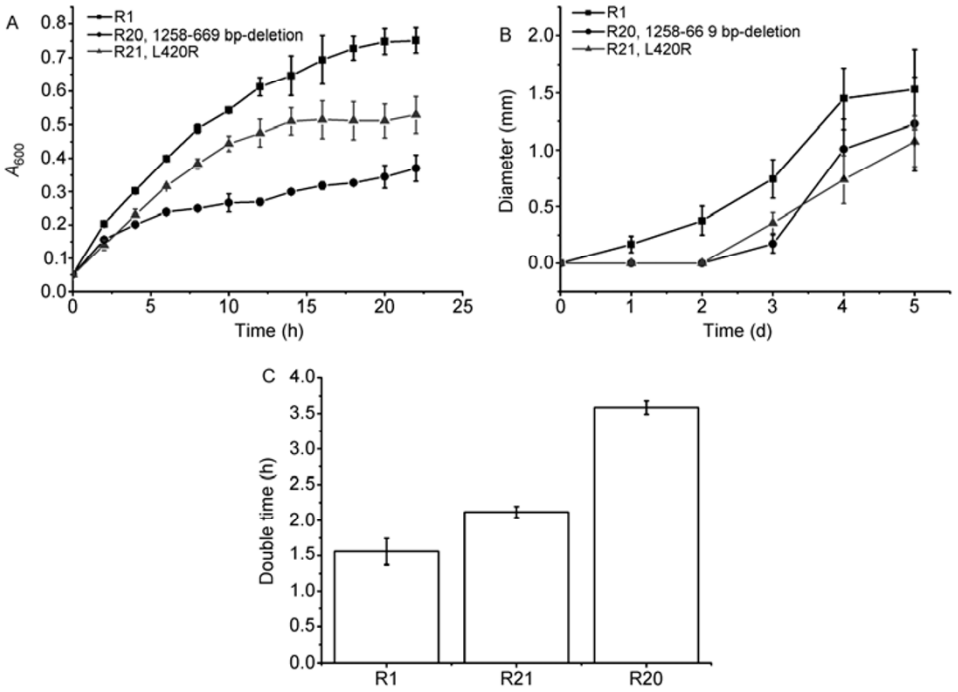

Figure 1 Growth of *D. radiodurans* and *rpoB* mutants in TGY medium. A, Growth curves were measured in a SPECTRAmax M5 microplate reader, as described in Materials and methods. Filled square, wild type; filled triangle, R20, 1258-66 9 bp-deletion; filled circle, R21, L420R. B, Clone sizes of *D. radiodurans* and its variants in TGY plates. Filled square, wild type; filled triangle, R20, 1258-66 9 bp-deletion; filled circle, R21, L420R. C, Doubling time of *D. radiodurans* and its variants in TGY medium. Data are expressed as average doubling times in hours±standard deviations.

els in the 9 bp-deletion *rpoB* mutant to that in the wild type via a microarray data package (Limma). The log *P*-value versus signal log ratio is shown in Figure 2. The horizontal line represents the *P*-value threshold ($P \leqslant 0.05$), and the two vertical lines represent the signal log ratio threshold (1.5 fold, signal log ratio, ±0.585). Genes with expression levels showing at least a ±1.5-fold change compared with wild type (signal log ratio, ±0.585) with $P \leqslant 0.05$ are shown in Figure 3. These genes are functionally categorized as indicated by the NCBI COG database. The 9 bp-deletion *rpoB* mutant showed down-regulation of 42 genes (Table 2). These genes are involved in cell wall/membrane/envelope biogenesis (M, 4 genes); metabolism, including inorganic ion transport and metabolism (P, 4 genes); amino acid transport and metabolism (E, 4 genes); transcription (K, 2 genes); poorly characterized genes (R, S, 5 genes); and other family and unclarified family genes (23 genes). Genes were also induced in the 9 bp-deletion *rpoB* mutant (Table 3). Seven genes are involved in metabolism: amino acid transport and metabolism (E, 5 genes), and coenzyme transport and metabolism (H, 2 genes). Four genes are involved in information storage and processing: Nucleoside triphosphate (NTP) pyrophosphohydrolases, including oxidative damage repair enzymes (LR, 2 genes) and transcription (K, 2 genes). There were 2 genes each involved in cellular processes and signaling: post-translational modification, protein turnover, chaperones (O) and cell wall/membrane/envelope biogenesis (M), respectively. There were 32 poorly characterized genes, which belonged to other families or unclarified families.

The majority of transcriptome alterations due to the 9 bp-deletion *rpoB* mutant seem to be related to slow growth and ROS accumulation. Therefore, we focused on the expression changes of three classes of genes involved in (i) metabolism, (ii) cellular processes and signaling and (iii) information storage and processing.

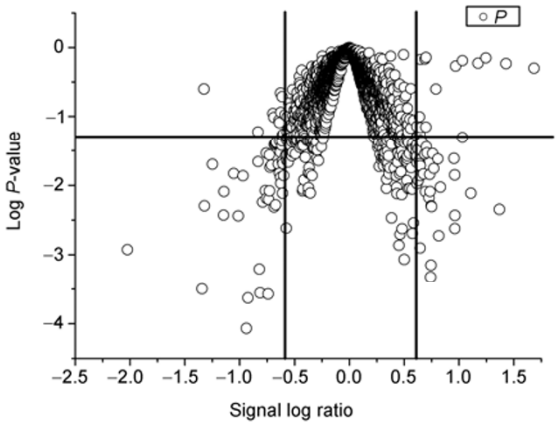

Figure 2 Global transcriptional changes in R20 compared with wild type. The log *P*-values are plotted against signal log ratios for R20. The horizontal line represents the *P*-value threshold ($P \leqslant 0.05$), and the two vertical lines represent the signal log ratio threshold (1.5 fold, signal log ratio, ±0.585).

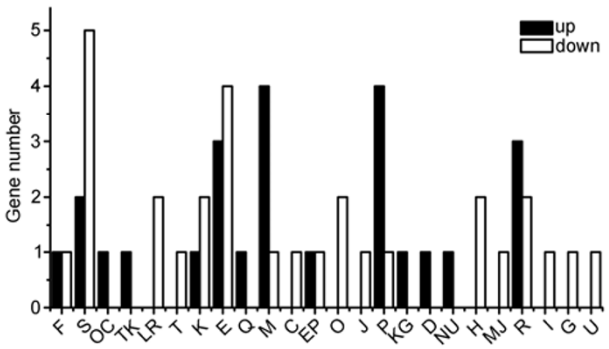

Figure 3 Genes whose expression levels changed >1.5-fold are functionally categorized according to data provided by the NCBI COG database. F, Nucleotide transport and metabolism; S, poorly characterized; OC, thiol-disulfide isomerase and thioredoxins; TK, response regulators consisting of a CheY-like receiver domain and a winged-helix DNA-binding domain; LR, predicted NTP pyrophosphohydrolase; T, signal transduction mechanisms; K, transcription; E, amino acid transport and metabolism; Q, secondary metabolite biosynthesis, transport and catabolism; M, cell wall/membrane/envelope biogenesis; C, energy production and conversion; EP, ABC-type dipeptide/oligopeptide/nickel transport system, ATPase component; O, post-translational modification, protein turnover, chaperones; J, translation elongation factors (GTPases); P, inorganic ion transport and metabolism; KG, transcriptional regulators of sugar metabolism; D, cell cycle control, cell division, chromosome partitioning; NU, flagellar biosynthesis pathway, component FlhB; H, coenzyme transport and metabolism; MJ, nucleoside-diphosphate-sugar pyrophosphorylase; R, poorly characterized; I, lipid transport and metabolism; G, carbohydrate transport and metabolism; U, intracellular trafficking, secretion, and vesicular transport.

Table 1 Strains used in this study

Strain	Description	Reference(s) or source
Deinococcus radiodurans		
R1	Wild type	ATCC
R20	As R1 but *rpoB*-(1258-66 9 bp deletion); Rif^r	This study
R21	As R1 but *rpoB*-L420R; Rif^r	This study
Escherichia coli TG1	*supE*, *hsd*Δ*5*, *thi*, Δ(*lac-proAB*)/F′ [*traD36*, $proAB^+$, $lac\ I^q$, *lacZ*Δ*M15*]	Takara

2.2.1 *Metabolism*

Iron is an essential nutrient for all organisms [25]. *D. radiodurans* has evolved various mechanisms to counter the toxicity and the poor solubility of iron, such as highly efficient iron acquisition systems and iron storage proteins [21]. We found that genes directly involved in iron transport were significantly repressed in the 9 bp-deletion *rpoB* mutant. These genes were involved in the iron ABC transporter system (*DRB0125* and *DRB0007*) and in the hemin transport system (*DRB0016*). These down-regulated genes related to iron transport suggested that the 9 bp-deletion *rpoB* mutant was under high-iron stress *in vivo*.

2.2.2 *Cellular processes and signaling*

Lipopolysaccharide is an essential component of the outer

Table 2 The 42 most highly repressed genes in the 9 bp deletion *rpoB* mutant

Locus	Annotation	Repression fold	
		Microarray	Q-RT-PCR
Cellular processes and signaling	Cell wall/membrane/envelope biogenesis		
DR2187	cyclopropane-fatty-acyl-phospholipid synthase, putative	2.075769	–
DRA0037	glycosyltransferase	1.897672	–
DRA0039	mannosyltransferase (mtfB)	1.757351	–
DRA0043	lipopolysaccharide biosynthesis protein, putative	1.525288	–
Metabolism	Inorganic ion transport and metabolism		
DRB0125	iron ABC transporter, periplasmic substrate-binding protein	2.016528	2.143547
DRB0016	hemin ABC transporter, ATP-binding protein	1.728907	–
DR2453	cation-transporting ATPase	1.700196	–
DRB0007	metal binding protein, putative	1.670389	–
Poorly characterized	General function prediction only		
DRA0038	rhamnosyltransferase, putative	1.916144	–
DRA0255	aculeacin A acylase (aac)	1.64962	–
DRA0331	conserved hypothetical protein	1.553765	–
Metabolism	Amino acid transport and metabolism		
DR2188	aminopeptidase	1.766147	–
DR1444	histidyl-tRNA synthetase, putative	1.545812	–
DRA0339	tryptophan 2,3-dioxygenase, putative	1.513616	–
DR1569	peptide ABC transporter, permease protein	2.207822	–
Poorly characterized	Function unknown		
DR1864	conserved hypothetical protein	4.064784303	–
DRA0153	conserved hypothetical protein	1.635929016	–
Information storage and processing	Transcription		
DR0005	conserved hypothetical protein	2.213661394	–
DR2296	glucokinase (glk)	1.531480259	–
Other families and unclarified families			
DR0751	conserved hypothetical protein	2.498705725	–
DR2117	adenylate kinase (adk)	1.52232904	–
DRA0291	2,4-dihydroxyhept-2-ene-1,7-dioic acid aldolase (hpcH)	1.528048514	–
DR1233	pilin, type IV, putative	1.586865817	–
DR0189	thiol:disulfide interchange protein (dsbE)	1.542621902	–
DR2091	chalcone synthase, putative	1.544172224	4.484664
DR0432	DNA-binding response regulator	1.656039721	–
DRA0103	hypothetical protein	2.537143753	–
DR0795	hypothetical protein	2.376044554	–
DRA0084	hypothetical protein	1.958607163	–
DR2323	transposase, putative	1.779816104	–
DR1249	hypothetical protein	1.689416671	–
DR0413	hypothetical protein	1.688394597	–
DR0162	hypothetical protein	1.665090696	–
DRC0021	hypothetical protein	1.657054181	–
DR2271	hypothetical protein	1.609158297	–
DRB0066	hypothetical protein	1.606834607	–
DR2228	hypothetical protein	1.60320038	–
DR0554	hypothetical protein	1.593591688	–
DR0665	hypothetical protein	1.592898716	–
DR1952	hypothetical protein	1.567578569	–
DR1448	hypothetical protein	1.555947405	–
DRA0292	hypothetical protein	1.532952731	–

Table 3 The 38 most highly induced genes in the 9 bp deletion *rpoB* mutant

Locus	Annotation	Induction fold	
		Microarray	Q-RT-PCR
Poorly characterized	Function unknown		
DR2270	conserved hypothetical protein	1.6542908	–
DR1314	conserved hypothetical protein	1.665161011	–
DR0973	gamma-carboxymuconolactone decarboxylase	1.661461029	–
DR0368	conserved hypothetical protein	1.617575985	–
DR0051	HesB-YadR-YfhF family protein	1.569182718	–
Metabolism	Amino acid transport and metabolism		
DR1410	carboxynorspermidine decarboxylase (nspC)	1.568820956	1.218410264
DR0873	O-acetylhomoserine (thiol)-lyase (cysD)	1.778610117	–
DR0872	homoserine O-acetyltransferase, putative	1.545311058	1.986184991
DR0365	peptide ABC transporter, permease protein	2.581385903	–
DR0777	3-dehydroquinate synthase (aroB)	1.525662882	–
Poorly characterized	General function prediction only		
DR1889	conserved hypothetical protein	2.155738671	–
DR0992	NADH oxidase	2.044651148	4.098227292
Cellular processes and signaling	Posttranslational modification, protein turnover, chaperones		
DR2325	serine protease, subtilase family, N-terminal fragment	1.670632997	–
DR2322	serine protease, subtilase family, C-terminal fragment	1.500425658	–
Information storage and processing	NTP pyrophosphohydrolases including oxidative damage repair enzymes		
DR0149	MutT-nudix family protein	1.565753752	–
DR0004	MutT-nudix family protein	1.567304636	–
Information storage and processing Transcription			
DRA0242	conserved hypothetical protein	1.569450974	3.282966435
DR0259	conserved hypothetical protein	1.957438671	2.799171731
METABOLISM	Coenzyme transport and metabolism		
DRA0121	aminotransferase, class III	1.627292819	3.063115994
DR0793	conserved hypothetical protein	1.532528502	–
Cellular processes and signaling	Cell wall/membrane/envelope biogenesis		
DR0710	mannose-1-phosphate guanyltransferase, putative	1.531852652	–
DR0487	conserved hypothetical protein	1.949956123	–
Other families and unclarified families			
DR1017	rRNA methylase	1.623459873	8.253465434
DR1189	methylmalonyl-CoA mutase, alpha subunit, chain A	1.583925673	3.810551992
DR0652	Na+-H+ antiporter, putative	1.543940486	–
DR1595	6-phosphogluconate dehydrogenase (gnd)	1.51652254	–
DR0584	formyltetrahydrofolate deformylase (purU)	1.632677218	–
DR2565	iron-sulfur binding reductase, putative	2.256151698	2.329467173
DR0805	conserved hypothetical protein	1.564262749	–
DR0510	sensory box protein	1.69257162	–
DR2027	hypothetical protein	1.947210289	–
DR1987	hypothetical protein	1.597816917	–
DR1818	hypothetical protein	1.67497681	–
DR1716	conserved hypothetical protein	1.532482447	–
DR1398	hypothetical protein	1.566112609	–
DR1211	hypothetical protein	1.610265294	–
DR1135	hypothetical protein	1.560067005	–
DR0858	hypothetical protein	1.937299343	–
DR0852	hypothetical protein	1.759642	–
DR0849	hypothetical protein	1.705804	–
DR0538	hypothetical protein	1.948329	–
DR0534	serine-threonine protein kinase-related protein	1.677419	–
DR0157	hypothetical protein	1.680944	–
DR0153	riboflavin-specific deaminase (ribD)	1.55544	–
DR0115	hypothetical protein	1.533483	–
DR0103	hypothetical protein	1.749987	–
DR0060	hypothetical protein	1.520016	–

membrane of Gram negative bacteria, and is present in high concentrations; approximately 10% of the total cell lipids [26]. Genes involved in cell wall/membrane/envelope biogenesis were repressed in the 9 bp-deletion *rpoB* mutant, including lipopolysaccharide biosynthesis protein (DRA0043). Lipopolysaccharide biosynthesis is essential for cell growth [27]. The repressed expression of lipopolysaccharide biosynthesis-related protein might cause slow bacterial growth.

2.2.3 Information storage and processing

Most organisms mainly metabolize glucose using the Embden-Meyerhof-Parnas (EMP) pathway, while the pentose phosphate (PP) pathway plays a minor role. The EMP pathway metabolizes about 80% of glucose, and the PP pathway consumes the remaining glucose in *Escherichia coli* [28]. The PP pathway plays an important role in preventing cell death and is usually very active in cells in highly oxidative environments [29,30]. The down-regulation of glucokinase (glk, DR2296) and the up-regulation of 6-phosphogluconate dehydrogenase (gnd) suggested that the EMP pathway was repressed and the PP pathway induced.

2.3 Consensus sequence for *D. radiodurans rpoB* dependent promoters

We analyzed the 300 bp sequence upstream of the up-regulated and down-regulated genes (Tables 2 and 3) using the program MEME to identify an *rpoB*-dependent promoter consensus sequence. A consensus sequence was determined from the up-regulated genes (Figure 4), but not from the down-regulated genes. The identified sequence was AT-rich.

2.4 Intracellular ROS levels were correlated with doubling time and MIC

We measured the ROS level in wild type and *rpoB* mutants. The ROS level in *rpoB* mutants was significantly higher than that in wild type. The 9 bp-deletion *rpoB* mutant showed a higher ROS level compared with the L420R *rpoB* mutant (Figure 5). Intracellular ROS levels of the three strains were correlated with doubling times and MICs of the strains.

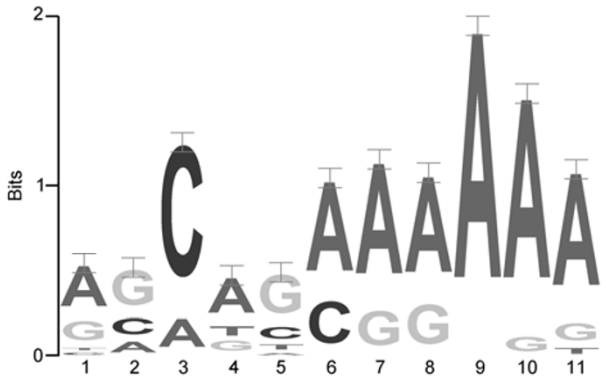

Figure 4 Weblogo depiction of the promoter sequences of genes which were induced in R20 compared with wild type as determined by MEME.

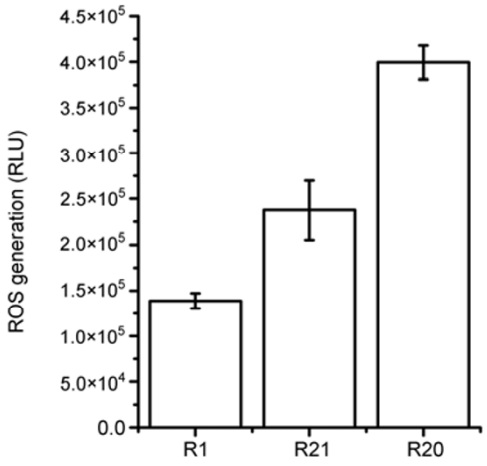

Figure 5 ROS generation in *D. radiodurans* and its variants. Data are the average and standard error of the mean of three independent experiments.

3 Discussion

We have previously investigated the mutation rates and spectra of spontaneous mutations in *D. radiodurans* under different rifampin stresses [14]. The isolated Rif^r mutants with higher rifampin MICs showed slow growth rates (Figure 1). Most types of antibiotic resistance impose a biological cost on bacterial fitness [31]. A genome-wide analysis of expression profiles would illuminate the mechanisms underlying the global effects of the 9 bp-deletion *rpoB* mutations on growth rate; therefore, in this study, we used DNA microarrays to investigate a mutation in *rpoB* that alters the global transcriptome in *D. radiodurans*.

The response of *D. radiodurans* to the 9 bp-deletion *rpoB* mutation was characterized, most notably, by the induction of genes that functioned in iron metabolism, cellular processes and signaling, as well as information storage and processing. The down-regulated iron-transport-related genes suggested that the 9 bp-deletion *rpoB* mutant was under high-iron stress *in vivo*. A state of high-iron stress was consistent with measurements of intracellular ROS levels. Higher ROS levels might cause single-strand breaks and DNA adducts, thus leading to lags in DNA replication. Induction of the PP pathway also indicated higher ROS level *in vivo*, since the PP pathway is usually very active in cells in highly oxidative environments [29,30]. The repressed expression of lipopolysaccharide biosynthesis-related protein might slow bacterial growth because of the lack of this important component of the outer membrane [27].

The increased level of ppGpp would lead to the inhibition of ribosomes and tRNAs by decreasing the lifetime of the *rrn* P1 open complex, leading to a higher amino acid

biosynthesis/transport promoter activity. RNA polymerase (RNAP) mutants that confer prototrophy to Δ*relA*Δ*spoT* strains, mimic the effects of ppGpp on wild-type RNAP. Mutant RNAPs formed shorter-lived open complexes than wild-type RNAP, similar to the effect of ppGpp on half-life [32]. The mutant RNAP in *D. radiodurans* might affect the global transcriptome through a decreased half-life of the open complex. The identified consensus promoter sequence of up-regulated genes in the 9 bp-deletion *rpoB* mutant was an AT-rich sequence. A-T base pairs have two hydrogen bonds (rather than the three formed in a C-G pair) and strands rich in these nucleotides are generally easier to separate [33]. A promoter containing an AT-rich sequence might have more chance to increase expression, because less time is spent on separating DNA strands to initiate transcription. However, we did not find a GC-rich sequence in the promoter sequence of down-regulated genes. The down-regulated mechanism of gene expression might be affected by the decreased half-life of the open complex and the expression of up-regulated genes. This hypothesis could be verified by an *in vitro* transcription experiment [10].

Transcription studies have focused on the regulatory roles of transcription factors and the sigma factor of RNA polymerase [34,35]. The components of the RNA polymerase core enzyme have largely been considered catalytic elements rather than regulatory elements. However, previous research has indicated that the RNA polymerase β-subunit plays an important role, not only in the catalytic aspect of transcription, but also in regulation of major developmental events in *Bacillus subtilis*. In this study, we used DNA microarray technology to investigate the molecular details that how the Rif^r mutations in the β-subunit led to the altered regulation of multiple genes. We compared the global transcription patterns in wild type versus the 9 bp-deletion *rpoB* mutant to identify novel up- or down-regulated genes in the Rif^r mutant. The phenotype of the 9 bp-deletion *rpoB* mutant was characterized by slow growth and ROS accumulation. This phenotype might be due to expression changes in three classes of genes encoding: (i) metabolism, (ii) cellular processes and signaling, and (iii) information storage and processing.

This work was supported by the National Natural Science Foundation of China (Grant Nos. 30830006 and 31000045), the National High Technology Research and Development Program of China (Grant No. 2007AA021305), Major Scientific and Technological Project for the Creation of Significant New Drugs (Grant No. 2009ZXJ09001-034), Major Project for Genetically Modified Organism Breeding (Grant No. 2009ZX08009-075B), and Application of Nuclear Techniques in Agriculture from Ministry of Agriculture of China (Grant No. 200803034) to Yuejin Hua, and the 2009 Zhejiang Innovation Program for Graduates. We thank Professors Junjie Fu and Zhiming Sun (Radiation Center of Zhejiang University) for their assistance in radiation treatment.

1 Garibyan L, Huang T, Kim M, *et al*. Use of the *rpoB* gene to determine the specificity of base substitution mutations on the *Escherichia coli* chromosome. DNA Repair (Amst), 2003, 2: 593–608
2 Kim M, Wolff E, Huang T, *et al*. Developing a genetic system in *Deinococcus radiodurans* for analyzing mutations. Genetics, 2004, 166: 661–668
3 Zeibell K, Aguila S, Yan S V, *et al*. Mutagenesis and repair in *Bacillus anthracis*: the effect of mutators. J Bacteriol, 2007, 189: 2331–2338
4 Tanaka M, Narumi I, Funayama T, *et al*. Characterization of pathways dependent on the uvsE, uvrA1, or uvrA2 gene product for UV resistance in *Deinococcus radiodurans.* J Bacteriol, 2005, 187: 3693–3697
5 Hua X, Huang L, Tian B, *et al*. Involvement of recQ in the ultraviolet damage repair pathway in *Deinococcus radiodurans.* Mutat Res, 2008, 641: 48–53
6 Liu X, Wu J, Zhang W, *et al*. Resistance of *Deinococcus radiodurans* to mutagenesis is facilitated by pentose phosphate pathway in the *mutS1* mutant background. Curr Microbiol, 2008, 57: 66–71
7 Mennecier S, Coste G, Servant P, *et al*. Mismatch repair ensures fidelity of replication and recombination in the radioresistant organism *Deinococcus radiodurans.* Mol Genet Genomics, 2004, 272: 460–469
8 Wehrli W, Knusel F, Schmid K, *et al*. Interaction of rifamycin with bacterial RNA polymerase. Proc Nat Acad Sci USA, 1968, 61: 667–673
9 Jin D J, Gross C A. Characterization of the pleiotropic phenotypes of rifampin-resistant *rpoB* mutants of *Escherichia coli*. J Bacteriol, 1989, 171: 5229–5231
10 Maughan H, Galeano B, Nicholson W L. Novel *rpoB* mutations conferring rifampin resistance on *Bacillus subtilis*: global effects on growth, competence, sporulation, and germination. J Bacteriol, 2004, 186: 2481–2486
11 Lai C, Xu J, Tozawa Y, *et al*. Genetic and physiological characterization of *rpoB* mutations that activate antibiotic production in *Streptomyces lividans.* Microbiology, 2002, 148: 3365–3373
12 Elisabetta C, Clelia P, Salvatore T, *et al*. Phenotypes and gene expression profiles of *Saccharopolyspora erythraea* rifampicin-resistant (rif) mutants affected in erythromycin production. Microbial Cell Factories, 2009, 8
13 Perkins A E, Nicholson W L. Uncovering new metabolic capabilities of *Bacillus subtilis* using phenotype profiling of rifampin-resistant *rpoB* mutants. J Bacteriol, 2008, 190: 807–814
14 Hua X T, Wang C, Huang L, *et al*. Mutation rate and spectrum of spontaneous mutations of *Deinococcus radiodurans* under rifampin stress. J Nucl Agric Sci, 2010, 24: 1166–1171
15 Kahnert A, Vermeij P, Wietek C, *et al*. The ssu locus plays a key role in organosulfur metabolism in *Pseudomonas putida* S-313. J Bacteriol, 2000, 182: 2869–2878
16 Mattimore V, Udupa K S, Berne G A, *et al*. Genetic characterization of forty ionizing radiation-sensitive strains of *Deinococcus radiodurans*: linkage information from transformation. J Bacteriol, 1995, 177: 5232–5237
17 Chen H, Huang L, Hua X, *et al*. Pleiotropic effects of recQ in *Deinococcus radiodurans.* Genomics, 2009, 94: 333–340
18 Rouillard J-M, Zuker M, Gulari E. OligoArray 2.0: design of oligonucleotide probes for DNA microarrays using a thermodynamic approach. Nucleic Acids Res, 2003, 31: 3057–3062
19 Smyth G K. Limma: Linear Models for Microarray Data. Bioinformatics and Computational Biology Solutions Using R and Bioconductor. New York: Springer, 2005. 397–420
20 Yang Y H, Dudoit S, Luu P, *et al*. Normalization for cDNA microarray data: a robust composite method addressing single and multiple slide systematic variation. Nucleic Acids Res, 2002, 30: e15
21 Smyth G K, Michaud J, Scott H S. Use of within-array replicate spots for assessing differential expression in microarray experiments. Bioinformatics, 2005, 21: 2067–2075
22 Bailey T L, Williams N, Misleh C, *et al*. MEME: discovering and analyzing DNA and protein sequence motifs. Nucleic Acids Res, 2006, 34: W369–W373
23 Crooks G E, Hon G, Chandonia J M, *et al*. WebLogo: a sequence logo generator. Genome Res, 2004, 14: 1188–1190
24 Gupta A, Rosenberger S F, Bowden G T. Increased ROS levels con-

tribute to elevated transcription factor and MAP kinase activities in malignantly progressed mouse keratinocyte cell lines. Carcinogenesis, 1999, 20: 2063–2073
25 Andrews S C, Robinson A K, Rodriguez-Quinones F. Bacterial iron homeostasis. Fems Microbiol Rev, 2003, 27: 215–237
26 Katz C, Ron E Z. Dual role of ftsH in regulating lipopolysaccharide biosynthesis in *Escherichia coli*. J Bacteriol, 2008, 190: 7117–7122
27 Onishi H R, Pelak B A, Gerckens L S, *et al*. Antibacterial agents that inhibit lipid a biosynthesis. Science, 1996, 274: 980–982
28 Gottschalk G. Bacterial Metabolism. 2nd ed. New York: Springer, 1986
29 Taccone-Galluci M, Lubrano R, Trapasso E, *et al*. Oxidative damage to RBC membranes and pentose phosphate shunt activity in hemodialysis patients after suspension of erythropoietin treatment. ASAIO J, 1994, 40: M663–M666
30 Pandolfi P P, Sonati F, Rivi R, *et al*. Targeted disruption of the housekeeping gene encoding glucose 6-phosphate dehydrogenase (G6PD): G6PD is dispensable for pentose synthesis but essential for defense against oxidative stress. EMBO J, 1995, 14: 5209–5215
31 Bjorkman J, Nagaev I, Berg O G, *et al*. Effects of environment on compensatory mutations to ameliorate costs of antibiotic resistance. Science, 2000, 287: 1479–1482
32 Barker M M, Gaal T, Gourse R L. Mechanism of regulation of transcription initiation by ppGpp. II. Models for positive control based on properties of RNAP mutants and competition for RNAP. J Mol Biol, 2001, 305: 689–702
33 Bramhill D, Kornberg A. A model for initiation at origins of DNA replication. Cell, 1988, 54: 915–918
34 Schmid A K, Howell H A, Battista J R, *et al*. Global transcriptional and proteomic analysis of the sig1 heat shock regulon of *Deinococcus radiodurans*. J Bacteriol, 2005, 187: 3339–3351
35 Schmid A K, Lidstrom M E. Involvement of two putative alternative sigma factors in stress response of the radioresistant bacterium *Deinococcus radiodurans*. J Bacteriol, 2002, 184: 6182–6189